# Wideband-CDMA for the UMTS/IMT-2000 Satellite Component

**Daniel Boudreau** (*I*), **G. Caire** (*II*), **G. E. Corazza** *(III)*, **R. De Gaudenzi** (*IV*), **G. Gallinaro** (*V*)**, M. Luglio** (*VI*), **R. Lyons** (*VII*), **J. Romero-Garcia** (*IV*), **A. Vernucci** (*V*), **H. Widmer** (*VIII*)

(*I*) Communications Research Centre (Canada), (*II*) Politecnico di Torino (Italy) now with EURECOM (France), (*III*) University of Bologna, Italy, (*IV*) ESA- ESTEC (Holland), (*V*) Space Engineering (Italy), (*VI*) Universita' di Roma Tor Vergata (Italy), (*VII*) Square-Peg Comm. Inc. (Canada), (*VIII*) Ascom Systec (Switzerland)

***Corresponding Author: R. De Gaudenzi***
***ESA-ESTEC (TOS-ETC), Keplerlaan 1, 2200 AG Noordwijk, Holland*** (e-mail: rdegaude@estec.esa.nl)

ABSTRACT

This paper describes the main aspects relevant to the development of a third-generation Radio Transmission Technology (RTT) concept identified as Satellite Wideband CDMA (SW-CDMA), which was submitted [1] for evaluation to the International Telecommunications Union (ITU) by the European Space Agency (ESA) in the framework of the International Mobile Telecommunications-2000 (IMT-2000) satellite-component standardization. The main outcomes of the extensive system engineering effort that have led to our proposal are described. In particular, we address propagation channel characteristics, satellite diversity, power control, pilot channel, code acquisition, digital modulation and spreading format, interference mitigation, resource allocation. Due to its similarity with respect to the terrestrial W-CDMA proposal, the SW-CDMA *open* air interface solution is described briefly, with emphasis only on the major differences. Quantitative results concerning the physical-layer performance over realistic channel conditions, for both forward and reverse link, are reported.

## 1. Introduction

In the general IMT-2000 standardization framework promoted by the ITU, the Universal Mobile Telecommunication System (UMTS) sponsored by the European Telecommunications Standardization Institute (ESTI) aims at the definition of a unified third-generation global wireless system operating in the 2 GHz band. UMTS is expected to support a wide range of connection-oriented and connectionless services with data rates up to 384 kbit/s in outdoor environments and up to 2 Mbit/s in indoor environments. The service bit rate can be negotiated at call setup and flexibly modified on a frame by frame basis. Through service and terminal classes definition, the standardization effort has identified the

core network functionalities that are air-interface independent. While the radio-independent core network will most likely encompass heterogeneous network technologies, radio technologies are being standardized in order to maximize the global system nature. A large effort is presently devoted to the selection of one or a few RTT (Radio Transmission Technology) proposals capable to efficiently support the IMT-2000 requirements.

The global IMT-2000 nature calls for service provision in a host of environments ranging from indoor pico-cells to satellite macro-cells. The fundamental satellite role in providing coverage over scarcely populated regions for true global roaming has been widely recognized in UMTS. For the first time the satellite is seen as an integral part of a cellular global communication network, although due to technological and physical constraints, satellite services can only represent a subset of those provided by terrestrial-UMTS (T-UMTS). Successful satellite integration within UMTS calls for the definition of an efficient, yet flexible, RTT well matched to the satellite mobile environment.

In this framework, ESA has undertaken a study on S-UMTS heading to RTT proposal and test-bed demonstration, the main results of which are summarized in this paper. The S-UMTS RTT definition has been performed with particular attention to the ongoing T-UMTS standardization activities in order to maximize commonality. Use of common S/T-UMTS technologies will in fact contribute to largely reduce dual-mode user terminals cost and size[1], thus boosting S-UMTS commercial opportunities. As known, the T-UMTS proposal encompasses two operationg modes: W-CDMA (wideband code division multiple access) associated with frequency division duplex, and TD-CDMA (time division – code division multiple access), associated with time division duplex. We considered both operating modes and adapted them to the satellite environment, which resulted in the two proposals identified as SW-CDMA (satellite wideband code division multiple access) and SW-CTDMA (satellite wideband code and time division multiple access) [1]. This paper focuses only on SW-CDMA for its more general applicability. As far as SW-CTDMA is concerned, suffice it to say that it may be a suitable solution for regional systems adopting geostationary or elliptical orbits. More details can be found in [1].

Commonality with T-UMTS is not the only reason for adopting CDMA in S-UMTS. As reported in [2], [3], the main drivers for CDMA selection are: higher capacity than TDMA in most situations, universal frequency reuse easing resource allocation, capability of satellite soft hand-off, exploitation of satellite diversity for improved quality of service and fading effects mitigation, MT (mobile terminal) moderate

[1] The cost/size reduction will be eased by the fact that T-UMTS and S-UMTS are allocated adjacent frequency bands.

EIRP (effective isotropic radiated power) requirements, applicability of interference mitigation techniques, flexible support of a wide range of services, provision of accurate user positioning, graceful degradation under loaded condition, simplified satellite antenna design[2], and compatibility with adaptive antennas. Finally, the low power spectral density nature of spread spectrum signals certainly helps in satisfying the respective regulatory constraints.

The SW-CDMA proposal has been devised independently from a specific orbit selection in order to represent as much as possible a global standard. However, being the focus on global systems, the adoption of low-Earth orbit (LEO) or medium-Earth orbit (MEO) satellite constellations seems most appropriate as they can be designed to allow almost global coverage of the populated regions with large probability of multiple satellite visibility. Also, from the acquisition and channel estimation point of view LEO orbits are the most demanding, and they can be considered as a benchmark. Therefore, the following discussion will assume the adoption of a LEO constellation, although the SW-CDMA RTT can be adopted for other system architectures as well.

The paper is organized as follows. In Section 2 we report the main system engineering considerations and trade-offs that have led to the SW-CDMA proposal. This is a rather unusual Section in that motivations behind standards choices are usually not reported in the open literature. The proposed SW-CDMA *open* air interface solution is described somewhat briefly in Section 3. Due to its similarity with respect to the terrestrial W-CDMA proposal, emphasis is placed only on the main characteristics and major differences, as for example the fact that we allow for the use of interference mitigation techniques on the mobile terminal. This is due to the fact that system capacity appears to be limited by the forward link (FL) and not by the reverse link (RL). Quantitative results concerning the physical-layer performance over realistic channel conditions, for both forward and reverse link, are reported in Section 4, where source coding for speech and video services is also considered. Finally, conclusions are drawn in Section 5.

## 2. System Engineering for SW-CDMA

In this Section we report the main system engineering considerations, trade-offs and analyses that have led to the proposal submitted to ITU. In particular, we address propagation channel characteristics and

[2] It can be shown that the average I/C (interference to signal power ratio) and not the worst-case I/C is the key antenna figure on top of gain.

blockage, satellite diversity, power control, pilot channel insertion, code acquisition, modulation and spreading format, interference mitigation, and resource allocation.

**A - Propagation channel characteristics**

As for any wireless system, channel characteristics play a key role in the definition of a S-UMTS RTT. Note that propagation conditions are quite different for LEO/MEO S-UMTS with respect to T-UMTS. In fact, the T-UMTS channel is typically affected by lognormal long-term shadowing and Rayleigh short-term multipath fading, with no line-of-sight (LOS) component, except possibly in pico-cellular environments. In these conditions the adoption of a rake receiver is certainly advisable, to detect and combine the strongest multipath components. Multipath diversity provides increased quality of service through fading mitigation and allows for soft hand-off. Conversely, due to the larger free space loss and on-board RF power scarcity, mobile satellite systems are forced to operate under LOS propagation conditions, at least for medium-to-high data rates. This results in a milder Rice (or at most Rice-lognormal) fading channel [2], with a Rice factor (the power ratio between LOS component and diffuse component) typically ranging between 7 to 15 dB [2]. Multipath diversity in a single satellite link cannot be exploited due to the fact that paths with differential delays exceeding 200 ns most often result to have insufficient power to be usefully combined by the rake receiver. Thus fading is effectively non-selective. Another major difference is that the *useful* dynamic range for the received signal power is much smaller than for terrestrial systems (for which it goes up to 80 dB). This is due to the different system geometry (reduced path loss variation within each satellite beam, in the order of 3-5 dB), and again to the limited on-board RF power which is insufficient to counteract path blockage. Path blockage can be induced by heavy shadowing from hills, trees, and buildings; the car's body, and the head of the user can also have a non-negligible impact. Tree shadowing can lead to 10-20 dB of excess attenuation and is often the cause for link outage. In essence, S-UMTS must operate in an *on/off* propagation channel, with Rice fading in the *on* condition [4]. Countermeasures to blockage-induced outage are essential to achieve satisfactory quality of service.

**B - Satellite diversity**

Satellite diversity is instrumental in our S-UMTS design, providing benefits in terms of reduced blockage probability, soft and softer-handoff capability, slow fading counteraction, and under certain conditions even increased system capacity. First of all, the intuition that the probability of complete blockage greatly reduces with the number of satellites in simultaneous view recently found confirmation in experimental

campaigns [5]. Figure 1 [6] shows how in a typical suburban environment the probability of blockage varies with the minimum elevation angle and the number of satellites in view. Reduced blockage translates immediately into improved quality of service. Note that the multiple satellites can be exploited very efficiently in a CDMA system adopting rake receivers to realize soft satellite-handoff and softer spot beam-handoff. CDMA also allows flexible allocation of diversity to different classes of terminals supported by IMT-2000. In fact, fixed or transportable terminals enjoying low blockage probability can be operated with almost no satellite diversity thus optimizing network resources exploitation.

Satellite diversity exploitation in the FL has a few differences with respect to the RL that are worth recalling. In the FL satellite diversity must be forced by the system operator by sending the same signal to different satellites through highly directive antennas. Note that the FL transmitted multiplex can adopt synchronous CDMA with orthogonal spreading sequences. Differently from the terrestrial case, the non-selective satellite fading channel preserves the CDMA orthogonality, thus minimizing intra-beam interference. It should be noted that forwarding the signal through different non collocated satellites somewhat increases the amount of inter-beam interference, thus causing an apparent capacity loss. However, in-depth FL system analysis for a multi-beam multi-satellite power controlled CDMA mobile system [6] showed that in practice, for a reasonable probability of single satellite blockage (e.g. 20 %, i.e. $p_b$=0.2), the overall system capacity multiplied by the probability of having at least one satellite in view (identified as normalized system capacity) is almost independent from the number of satellites providing path diversity (see Figure 2). For $p_b$=0.4 satellite diversity provides even larger normalized system capacity.

Assuming transparent transponders, exploitation of satellite diversity in the RL is practically unavoidable due to the MT quasi-omnidirectional antenna. Universal frequency reuse allows for *satellite antenna arraying* (similar to Deep Space probes ground reception techniques) whereby the different replicas of the same user terminal signal transponded by the different satellites are independently demodulated, time aligned and coherently combined at the gateway station. This detection technique, requiring a rake receiver, results in a drastic reduction in the user terminal EIRP even under LOS conditions.

As noted in the previous subsection, multipath diversity cannot by exploited in S-UMTS, and this fact can seriously affect the link budget especially for slow moving MTs. Once more, satellite diversity comes in to yield very significant gains even in the presence of slow fading. This is extremely important as the slow fading is neither counteracted by power control (characterized by very slow dynamic capabilities) nor by the finite size interleaver. For mobile satellite systems slow fading represents the most power

demanding link condition. With satellite diversity it is possible to largely counteract these adverse slow fading effects with very modest power margins.

**C - Power control**

Considerable attention has been devoted to a fundamental issue for any CDMA system: power control. In fact, although the near-far effect in S-UMTS is not as bad as for T-UMTS, power control must necessarily be implemented in order not to waste precious power and system capacity. Slow (trackable) power level variations are due to different causes such as satellite motion[3] (path loss changes), satellite and user antenna gain variations, shadowing, user speed changes, time varying co-channel interference. As in T-UMTS, a combination of open-loop for random access channels and closed-loop power control for connection-oriented channels is required. Due to the longer satellite propagation delay, closed-loop power control is slower and less responsive to fast dynamics as compared to T-UMTS, and as such its design is critical. In the following we dwell on the implementation of closed-loop power control in SW-CDMA.

Based on the CDMA terrestrial system (IS-95) experience, closed-loop power control can be based on two loops working concurrently to provide the desired Frame Error Rate (FER). The *inner* loop is used to adjust the channel SNIR[4] (signal-to-noise-plus-interference ratio) to the target SNIR which is needed to achieve the target FER. Note that the target SNIR depends on the propagation environment, user speed, path diversity conditions, all of which change dynamically. Therefore, an *outer* loop is needed to adapt the target SNIR to match the measured FER to the target FER. However, to cope with the increased propagation delay in satellite links, algorithm modifications are required in terms of (a) optimization of power control command (PCC) rate, (b) SNIR estimation, and (c) mechanization of the inner loop.

Concerning point (a), due to the propagation delay the PCC rate should be reduced to one per frame (10/20 ms, as shown later), as opposed to one per slot as used in T-UMTS. This avoids over-sampling and possible loop instabilities, without affecting the frame structure regularity. Another important point is to keep memory of the last PCCs sent, but not yet received because of propagation delay, before deciding for a new PCC. In this way, power control tracking of slow variations becomes rather insensitive to the satellite orbital height.

---

[3] This effect tends to be compensated by the so-called iso-flux antenna design that attempts to equalize the geometry dependent path loss with antenna gain shaping.

[4] After rake combing and interference mitigation if applicable.

As for point (b), SNIR estimation can be performed on the total received signal, or on known reference symbols if available (data-aided). In the absence of reference symbols, two options are available: use tentative, or final, data decisions to remove modulation or use a non-linear transformation to recover an unmodulated signal component, which can be used in place of the reference symbols. In both cases, a bias in the estimate occurs at low SNIR, which however can be compensated for by the outer loop. The variance of the SNIR estimator is more important, and as expected the best results are achieved with the data-aided approach, at the price of some resource expenditure. The latter approach has been selected in SW-CDMA.

Concerning point (c), a four level inner-loop mechanization can be shown to provide the best tracking performance in most situations. The four levels correspond to small/large, positive/negative steps. The small step is well suited to track, with minimum jitter, "regular" changes in antenna gain or path loss and slow shadowing, while the large step is best suited to recover sudden changes in the received SNIR. The following parameters appear to be a good compromise: small step for SNIR errors less than 2 dB: $\Delta_1^{PC}$=0.2 dB, large step for SNIR errors greater than 2 dB: $\Delta_2^{PC}$=1 dB. Figure 3 and Figure 4 show the response to a step attenuation and to a sinusoidal attenuation variation superimposed on slow Rice fading. In both cases the loop corrections (thin line) appear to well counteract[5] the "slow" channel attenuation variations (thick line). Further, Figure 5 shows that the performance of power control is quite insensitive to the actual loop delay. This result was obtained for a two-level loop but applies also to the four-level loop.

Finally, we want to quantitatively confirm the limitations and capabilities of power control in S-UMTS. Table 1 shows the average SNR needed, with and without power control, in the presence of fast Rice fading superimposed to a slow sinusoidal shadowing (±5 dB or ±10 dB peak-to-peak). The simulation results confirm that in S-UMTS power control is unable to track fast power variations, and as such there are no gains in average requested SNR with respect to non-power controlled system. However, if power control is not implemented the requested SNR must be achieved through the use of static link margins, which must therefore be sized for the worst case attenuation. Instead, adaptive power control is capable to detect unacceptable link quality of service and promptly correct for it with an adequate average power increase *only when it is required*. In essence, power control is essential in S-UMTS systems to avoid capacity degradations induced by the use of static link margins.

[5] Note that in case of sinusoidal power variations for plot clarity the inverse of the power control gain plotted against time.

**D - Pilot channel**

A pilot channel is useful in both FL and RL. Considering the FL, first note that the (fast) satellite motion in LEO/MEO/HEO constellations generates a remarkable Doppler effect that must be accounted for in the system design. The main Doppler impact is the need for special measures for initial signal acquisition and carrier tracking. Most of the Doppler can however be pre-compensated for[6] thus reducing the frequency uncertainty. To ease initial pseudonoise sequence synchronization, it is expedient to include in the satellite FL a common pilot, which can also be used to achieve coherent detection and to initially adjust power level in return direction (open-loop power control). Also time domain multiplexing of pilot symbols (TDMP) in the different data streams in pre-assigned time slots is possible to support adaptive satellite antennas.

In the RL a pilot can be paired to each information signal. The reduction in power level (around 10-20% power on pilot is typical) is balanced by the benefit of coherent detection at the gateway [7]. Code division multiplexing of an auxiliary channel carrying pilot symbols and signaling information (rate information, power control bits) (CDMP) was found preferable from the system perspective. In the RL, pilot-aided code division multiple accessed quasi-coherent uplink was found to provide a gain higher than 1 dB compared to the 64-WH modulation even at very low symbol rates (up to 2.4 kbit/s) [7]. The in-quadrature pilot symbols insertion (together with control channel bits) allows to independently transmit variable rate traffic from control signaling and pilot symbols with reduced envelope fluctuations.

**E – Code acquisition**

In the FL, the system must guarantee efficient initial code acquisition at the mobile terminal, both for login into the system and for soft hand-off handling. As pointed out in the previous subsection, a common pilot tone can be introduced for this purpose. The pilot tone can be in the form of a continuous waveform (CW) spread by a long PN code, as in IS-95, or as a Burst Pilot (BP), where all the pilot energy is concentrated in a fraction, *d*, of the available slot time, identified as the *duty cycle*. Evidently, for the same average pilot power, the peak power for BP is *1/d* times higher than for CW. We analyzed both approaches, adopting various versions of the MAX/TC (Maximum/Threshold Crossing) criterion [8] to drive the acquisition subsystem. In all cases, non coherent post-detection integration is needed to achieve sufficient SNR to make reliable decisions. Also, a single dwell architecture was assumed for simplicity. Figure 6 shows the mean time to acquisition using the TC criterion for the FL pilot evaluated as a

[6] At least for feeder link part (satellite-to-gateway) and for the downlink center-of-beam.

function of the chip energy to thermal noise density, Ec/No. The computation assumes that the user is at the cross-point of three equal loaded beams and that in each beam only 3.3% of the beam power is dedicated to the pilot. A frequency error of 20 kHz was considered. To cope with the frequency error a matched filter processor has been considered with a parallel frequency search through the use of the swivelled FFT concept [9]. Figure 6 shows a definite advantage for the BP solution, which can be explained by the fact that, assuming equal dwell time for BP and CW, more energy is integrated *coherently* in the BP case. However, it can be shown that allowing for a longer non coherent post-detection integration in CW (approximately double with respect to BP) the same detection probability can always be achieved. In essence, there is a trade-off [10] between acquisition time (which is in favor of BP, but not dramatically) and hardware complexity and resilience to non-linearity (which are in favor of CW). In our system simulations, reported in Section 4, we have adopted the BP approach.

Coming now to consider the RL, the main difference is that no pilot can be permanently transmitted for acquisition purposes. Initial code acquisition shall instead be performed on a single ad-hoc preamble, which is transmitted only once. Furthermore, a TC strategy should be adopted (a MAX strategy requires that there is always a right hypothesis to detect[7]), and sophisticated multiple-dwell algorithms cannot be exploited. Another important difference is that more hardware complexity can be supported in the gateway. Again frequency errors and possibly timing errors must be faced. A strategy, similar to the FL approach, is to coherently integrate on a partial number of chips, and then complete by non-coherent integration. An alternative strategy is to substitute non-coherent integration, with differential integration. A comparison between the two strategies, in terms of false alarm probability and missed detection probability, is shown in Figure 7. It appears that differential integration yields the best results, and this was adopted in our simulations.

**E - Digital modulation and spreading format**

A large effort has also been devoted to the optimization of modulation and spreading format. For the FL three options were considered: (option Q) QPSK modulation with binary Walsh-Hadamard (WH) spreading and real binary scrambling; (option D) dual BPSK with WH spreading and complex scrambling; (option IQ) BPSK modulation and WH spreading, half of the user carriers being transmitted on the in-phase channel and the other half on the quadrature channel, I and Q scrambled by two different

[7] An ML strategy could be adopted, if the presence of the burst has been previously detected with another strategy [11].

codes. An asymptotic analysis has been performed using both a conventional correlation receiver, also identified as single user matched filter (SUMF) receiver, and an ideal interference suppressing linear minimum mean square error (LMMSE) receiver. Implementation of interference mitigation in S-UMTS will be described in more detail in the next section. In both cases ideal coherent detection is assumed. Results are given in Figure 8 where the cumulative distribution for SNIR obtained at the receiver output is shown. The nominal SNR (thermal noise only) is 6 dB in all cases. Both double-diversity (thick lines) and triple-diversity (dotted lines) with maximal ratio combining was considered, with each satellite carrying the same K number of users (all at equal level). The spreading factor considered for IQ was 64. For Q and D, the spreading code length is actually doubled, due to the longer symbol interval. Note that for SUMF the three schemes achieve the same average SNIR. However, the SNIR distribution for D has slightly shorter tails than that for Q, while IQ has the longest tails. With an LMMSE receiver Q performs significantly better than D and IQ, the advantage increasing with the number of users. The reason being that Q has a double spreading code length with respect to IQ and requires half of the number of codes required by D. A remarkable result is that triple satellite-diversity provides better SNIR under light loading conditions, whilst in high loading conditions the best SNIR is achieved with double-diversity. In our proposal, the Q option was selected for data rates larger than 4.8 Kb/s. For very low-data rates (i.e 2.4 Kb/s) BPSK was retained as simulations indicated its superiority when channel estimation errors and user terminal phase noise is considered.

**F - Interference mitigation**

For a multi-satellite SW-CDMA system the capacity bottleneck is represented by the FL. This is due to the limited satellite RF on-board power available which hurts FL capacity, and to the (quasi)-permanent uplink soft handoff conditions that increase RL capacity. This explains our interest for robust decentralized CDMA interference mitigation techniques that can be applied to the mobile user terminal thus reducing average FL power consumption. Among the different CDMA interference mitigation techniques, the blind Minimum Output Energy (MOE) solution [12], [13], [14] appears particularly suited for use in a decentralized single detector implementation because of the affordable complexity increase compared to the conventional correlation receiver (CR) [15]. Nonlinear schemes were discarded for their complexity not suited for a single user terminal, and sensitivity to channel estimation errors. More precisely, the scheme investigated was the Extended Complex Blind Adaptive Interference Detector

(EC-BAID) [14] featuring extended observation window, rotationally phase invariance[8] and insensitivity to interferers frequency offset. Both LMS (Least Mean Square) and RLS (Recursive Least Square) EC-BAID adaptation schemes were simulated. However, the RLS version suffers from a much greater implementation complexity compared to LMS. The marginal RLS advantage over LMS provided in AWGN channel was found to be superseded by the superior LMS performance over fading channels [3]. The LMS version is the one considered in the numerical results.

**G - Resource allocation**

An important system issue is the selection of a strategy for resource allocation in a system using a satellite constellation and in which satellite beams can overlap. This issue must be seen in conjunction with the potential advantages provided by MOE adoption. Three different strategies have been considered for FL resource assignment:

1) Avoid frequency reuse among overlapping satellites adopting CDMA/FDMA multiplexing, 2) Full frequency reuse among all beams of all satellites without applying permanent satellite diversity[9], 3) Full frequency reuse among all beams of all satellites applying permanent satellite diversity (soft hand-off).

Clearly option 1 is the one minimizing mutual satellite interference at the expense of the occupied bandwidth. In fact, when no frequency reuse among satellites is implemented, then FDMA satellite multiplexing implies an increased bandwidth occupancy compared to a full frequency reuse scenario. Option 2 avoids the CDMA/FDMA bandwidth increase at the expense of an increased inter-satellite CDMA self-noise[10]. Option 3 combines the frequency reuse advantage of option 2 with the artificial path diversity generation achieved by using multiple satellites, as described previously. Disregarding blockage effects, semi-analytic simulation results for the case of slow-fading encountered by hand-held terminals have been performed in [16]. Considering as a figure of merit the number of active users/frequency slot/beam/satellite, which accounts for both power and spectral efficiency, it has been found that option 3 is preferable for both CR and MOE detectors while the adoption of MOE detectors instead of a CR provides a 110 % capacity increase for option 2, 60 % for option 1 and 50 % capacity boost for option 3. The MOE advantage will be even more important in a practical system whereby power control errors will enhance the multiple access interference effects.

---

[8] Allowing for carrier phase removal after the adaptive detector.

[9] Temporary satellite path diversity can be envisaged during satellite hand-off.

[10] It should be recalled that for an individual satellite the intra-beam self-noise is eliminated by the adoption of O-CDMA.

## 3. SW-CDMA vs. Terrestrial W-CDMA specifications

As repeatedly stated, SW-CDMA represents an adaptation of the T-UMTS W-CDMA proposal [1]. For this reason only the main SW-CDMA features and deviations from W-CDMA will be discussed here[11].

### A - Chip rate

In SW-CDMA, two chip rate options are supported: a 4.096 Mchip/s option and a half-rate option at 2.048 Mchip/s, which may be more suitable in a multi-operator environment where bandwidth limitations may arise.

### B – Channelization and scrambling codes

As in W-CDMA, FL channelization is based on the orthogonal variable rate spreading factor (OVSF) codes [17] to accommodate different data rates while maintaining orthogonality. OVSF codes efficiently support frame-to-frame variable bit rates without requiring an increase in demodulator hardware complexity (no need for multi-code correlators for higher data rate services). OVSF are also used in the RL to multiplex the various data and signaling channels transmitted by the user. A major difference with respect to W-CDMA is the optional use of a short randomization (scrambling) code[12] (an extended Gold-like codes of length 256 chips) to try to exploit the benefits which arise from the use of adaptive linear interference mitigation techniques, as discussed in the previous Section.

### C – Logical channels

The set of logical channels used in SW-CDMA and the supporting physical channels are listed in Table 2. The logical channels are the same as those defined in Recommendation ITU-R M.1035 apart for the Layer 1 Signaling channel. This logical channel has the purpose to support coherent demodulation, power control functions and data rate agility. It is mapped to the Dedicated Physical Control CHannel[13] (DPCCH) and is always associated (via time or code multiplexing) to at least one Dedicated Physical Data Channel (DPDCH).

---

[11] The T-UMTS specifications are still evolving, so the discussion here refers to the IMT-2000 T-UMTS submission.

[12] A slot length (2560 chips) longer randomisation code, instead of frame length, is proposed in case no forward link mitigation techniques are adopted.

[13] The logical Dedicated Control Channel (DCCH) which has the purpose to support layer 2 and higher signalling functions is instead multiplexed with the Dedicated Traffic Channel (DTCH) on the same DPDCH.

The Common Control Physical Channels (CCPCH) is available on the FL. In particular, a Primary CCPCH will carry the Broadcast Control CHannel (BCCH) as well as reference symbols to support initial acquisition, coherent demodulation and time ambiguity range extension as necessary for supporting satellite diversity operation on the FL. The primary CCPCH has a fixed transmission rate (16 kbit/s in the full chip rate option and 8 kbit/s in the half chip rate option). To support time ambiguity range extension for satellite diversity operation, a Unique Word (FSW) is modulated on some of the reference symbols carried by the DPCCH (see Figure 9).

Initial FL acquisition is performed on a burst pilot by means of ad-hoc unmodulated reference symbols inserted in the primary CCPCH at the beginning of each time slot. Hence, even in case the long scrambling code option is selected, always the same 256 chips are used by such reference symbols. The transmission level of these reference symbols is typically higher than the other symbols in the Primary CCPCH to facilitate initial acquisition.

**D – Frame structure**

Figure 10-a shows the FL frame structure for the DPDCH and DPCCH; the two logical channels are time multiplexed within the frame. The frame length is 10 ms or 20 ms when the half chip rate option is adopted. The FL modulation and spreading adopts QPSK modulation with binary spreading and scrambling codes (see Figure 11), as per our system engineering study. Also, Transmit Power Control (TPC) bits are coded together with Frame Control header (FCH) bits using a bi-orthogonal code spanning the whole frame. Hence, the up/down power control commands rate is reduced compared to W-CDMA to a single command/frame. Figure 10-b shows the frame structure for the RL DPDCH and DPCCH logical channels. Being modulated on the I-Q channels separately and at different bit rate, no logical channels time interleaving within the frame is required. The RL modulation and spreading format is depicted in Figure 12. Similarly to T-UMTS the DPDCH and the DPCCH are code multiplexed and phase multiplexed. This approach, combined with complex scrambling helps in reducing carrier envelope fluctuation even with unbalanced I and Q power level.

**E – Packet service**

In the FL, packet traffic is supported either on the FACH channel for sporadic packets or on a dedicated traffic channel for bulky packet traffic. The main advantage of this approach is that the closed loop power control can be kept active during the inactive time slots thus minimizing packet services interference to the other active channels in the same frequency slot. In the RL, the RACH channel may be utilized for the

transmission of occasional short user packets, mapped onto the Physical Random Access CHannel (PRACH). The PRACH is composed by a 48 quaternary symbol preamble and a data part whose length is one frame (Figure 13). The preamble part is spread by a binary code which is randomly selected between a limited set of codes for random access. The usable set of codes is communicated on the BCCH channel. The PRACH burst data part is actually composed of a data channel on the I transmission arm and an associated control channel on the Q transmission arm carrying the reference symbols for coherent demodulation and a FCH informing about the data rate and format of the I arm. The PRACH burst data part spreading is complex and similar to the spreading of normal dedicated carriers. The I and Q codes used are univocally associated to the binary code used for spreading the preamble. For a non-occasional, but still moderate throughput and/or low duty cycle packet traffic, ad hoc codes will be assigned by the gateway to the user, in order to avoid code collision with other users of the RACH channel. In this case, the RTCH (Random Traffic Channel) is still mapped on a RACH-like physical channel. The data part, however, may be of variable length (in any case a multiple of the physical layer frame length). For higher throughput packet channels on the RL, a couple DPCCH/DPDCH can be assigned. The DPDCH is only transmitted when the packet queue is not empty. In this case, in addition to the advantage of keeping the closed-loop power control active during packet bursts, the channel allocation approach allows to keep full channel synchronization.

## 4. Physical layer and source coding performance simulation

A complete physical layer simulator program was developed to accurately simulate the proposed RTT performance. Considering the high SNR affecting the feeder links (gateway-satellite link) only the user links (i.e. from satellite to user and vice-versa) have been modeled. The simulator is capable to simulate both the FL and the RL. The following aspects of the physical layer have been modeled: signal framing structure, FEC coding and puncturing, interleaving, modulation and spreading (for traffic and signaling channels), CDMA interference (from the various satellites), channel impairments (High Power Amplifier (HPA) non-linearity, carrier/code Doppler, phase noise, fading), satellite diversity, multi-rate rake demodulators (inclusive of initial acquisition, chip tracking, frequency, phase and amplitude estimators, CDMA interference mitigation, de-interleaving FEC decoders). Only a few aspects of the real system have not been included in the simulator due to their excessive impact on the required simulation time. The most notable omission is the power control loop. Validation of the power control loop was performed with a different simplified ad-hoc simulator, the results of which have been discussed in Section 2. When

not mentioned otherwise, the 2.048 Mchip/s chip rate was used. In all cases, flat Rice fading channel with a Rice factor of 10 dB was assumed. Two different user speeds were considered: 70 Km/h and 3 Km/h, corresponding respectively to Doppler spreads of 140 Hz (*fast fading*) and 6 Hz (*slow fading*) assuming operation in the 2 GHz IMT-2000 band. In addition, the physical layer simulator was coupled to various traffic generators to perform an end-to-end source coding simulation.

## A - Forward link physical layer performance

The FL simulator can account for multiple satellites. For each satellite, multiple beams can be generated. For each beam, the simulator generates a primary CCPCH and a variable number of traffic channels, i.e. couples of DPDCH and DPCCH (see Section 3). Each resulting multi-beam satellite signal is fed to a HPA[14] and then to a channel simulator generating independent fading for each satellite path and noise. The signals transponded by the different satellites are then combined together at the demodulator input. Simulations were performed with either optional reference symbols included in the DPCCH for channel estimation (this being mandatory in case adaptive antennas are used on-board) or without such reference symbols, this option being more efficient in presence of fixed beams. The latter solution, which exploits the reference symbols on the primary CCPCH for channel estimation, not only allows to save on-board power (by not transmitting unnecessary reference symbols in each dedicated carrier), but also reduces the interference level[15]. Moreover, better channel estimation is often possible by exploiting the CCPCH reference symbols instead of those embedded in the DPCCH because of the typically larger power of CCPCH reference symbols. In the following results, we will assume that the DPCCH takes the 20% of the overall time slot length in case the optional reference symbols are transmitted. In that case the DPCCH consists of one reference symbol and one TPC/FCH symbol per slot. In the absence of the optional reference symbols, the DPCCH takes instead 10% of the time slot (only one TPC/FCH symbol per slot is transmitted). Even when reference symbols are included in the DPCCH, we have assumed that frequency tracking is still performed on the CCPCH. An AFC bandwidth of 6 Hz and a channel estimation window of 6 time slots (7.5 ms) were assumed. No case-by-case optimization of the reference symbol power level was done. If not stated otherwise, reference symbols are transmitted at a relative level

[14] It has been shown in Ref. [18] that the single HPA represents a worst-case modeling of the on-board nonlinearity effects experienced by a CDMA signal flowing through an active phased-array antenna.

[15] Reference symbols are typically transmitted at a higher power level with respect to information data symbols causing burst of higher interference power.

(with respect to other symbols in the carrier) of +6 and +4 dB respectively for the primary CCPCH and the DPCCH while TPC/FCH bits are using the same level as the DPDCH. With this assumption, an overhead of 1.58 dB or 0.46 dB results due to the usage of the DPCCH, respectively in the options with and without reference symbols. For the FEC, the standard rate $r$=1/3 or 1/2, constraint length $k$=9 convolutional codes have been adopted. Suitable bit puncturing or repetition is used to fit the encoded bit stream to the frame structure. Finally channel interleaving over a single frame (20 ms. in the 2.048 Mchip/s rate option here considered) is assumed.

Results are typically given as a function of the ratio between the single path bit energy $E_p$ and the thermal noise density $N_o$, where the bit energy per path $E_p$ also includes the overhead due to the DPCCH. It must be stressed that $N_o$ only accounts for thermal noise. Clearly for the same $E_p/N_o$, the actual performance will strongly depend, in addition to the propagation channel conditions, also on the Multiple Access Interference (MAI) level. A first set of simulations was aiming at verifying the performance of a conventional correlation receiver CR under the two fading scenarios previously discussed with and without satellite path diversity. A second set of simulations was aimed at verifying the potential gain coming from the adoption of the MOE interference mitigating receiver. Finally the impact of on-board non-linearity was assessed.

**Conventional Correlation Receiver (CR)**

Figure 14 and Figure 15 report the CR simulations results for 8 kbit/s channels in *fast* and *slow* fading for single and dual diversity. The basic code rate is 1/3 (k=9); hence, assuming the use of an 8-bit CRC plus 8-bit tail at the end of each frame, 528 bits would be available at the output of the convolutional code. Some bit repetition is thus used to fill the frame (576 bits total available). No dedicated reference symbols are used. It shall be observed that the number of traffic carriers used in the simulation takes into account that with double diversity, the overall number of DPDCH/DPCCH to be transmitted shall double to maintain the same traffic level. Nevertheless, double diversity provides a consistent advantage (especially for the slow fading case) even when the total $E_b/N_o=E_p/N_0+3$ dB is considered in lieu of the *per finger* $E_p/N_o$. Hence it can be concluded that satellite diversity provides increased capacity (for typical fading scenarios) even disregarding link blockage probability.

The peculiar nature of the FL CDMA interference has an impact on the way CDMA self-noise behaves. Figure 16 compares the simulated FL BER in the presence of the actual CDMA self-noise versus the equivalent $E_p/(N_0+I_0)$ computed using the standard Gaussian approximation for the MAI for a scenario

with slow fading and double diversity. This plot can be compared with the one obtained replacing the background FL MAI with an equivalent white Gaussian noise generator. The realistic system simulation shows about 1.5 dB better performance than that predicted by the AWGN MAI model for the case of dual diversity with slow fading. Other simulations, also including reference symbols in the DPCCH, showed an even higher difference in performance (more than 2 dB). It follows that the FL CDMA interference cannot be assimilated to thermal noise in the presence of slow fading. This fact is explained by considering that for each satellite, channel fading affects in the same way the wanted and interfering channels. Hence, during fading, the instantaneous $E_b/N_0$ decreases while the $E_b/I_0$ due to the other satellite beams remains constant thus the overall $E_b/(N_0+I_0)$ fluctuation due to fading is mitigated. Simulation results for fast fading (not included here) show that in this case the AWGN MAI model is adequate.

**Blind MOE Receiver Performance**

As previously mentioned, the linear blind MOE receiver with LMS adaptation was selected for possible use on the FL. Although theoretical and simulation results on Blind-MOE receiver performance also including some static channel estimation error were already available in the literature [14], none of them was representative of a heavily coded multi-rate CDMA rake adaptive demodulator exploiting path diversity. It is in fact known that demodulator operations at low SNR due to the powerful FEC scheme selected are in favor of the CR. The following performance of the Blind–MOE receiver have been obtained in a realistic[16] FL multi-beam multi-satellite scenario taking into account also the peculiarities of the access scheme and the effect of non ideal signal parameter estimation. A short randomization code (256 chips) was employed. It shall be observed that the selected randomization code period is still longer than the data symbol (at least for bit rate exceeding 4.8 Kbit/s). The blind MOE receiver in this case has to be implemented as a set of independent receivers each working on a different sub-interval of the randomization code period. It can be found that the adaptation speed of the algorithm is almost independent of the data rate.

Some interesting causes of performance degradation have been discovered. One of the peculiarities of the proposed access scheme is the non constant-envelope of the traffic channel, particularly when reference symbols are embedded in the DPCCH associated to each DPDCH. The presence of this amplitude

[16] One of the main deviations from reality is represented by the lack of power control level adjustment of the different forward link channels. This issue has been rigorously tackled in [16].

variations makes the performance of the blind MOE somewhat sub-optimum compared to those achievable with constant envelope. It was also found that fixed reference symbols, or other possible repetitive patterns, lead to a correlation between interference and wanted carrier that may occasionally strongly degrade the MOE receiver performance. Consequently, if reference symbols cannot be avoided, a scrambler to randomize carrier data (including reference symbols in the DPCCH associated to each DPDCH) is mandatory for compatibility with the use of the blind MOE technique. An additional degradation comes from the delay-lock loop (DLL) tracking error. In addition to the DLL timing jitter a bias in the recovered timing is inherent in the use of short spreading codes **[19]** as required by the adoption of Blind MOE adaptive detectors. The bias is typically more pronounced in the FL than in the RL due to the chip synchronization between different channels belonging to the same satellite. Moreover, it is typically worse in a scenario were the number of intra-beam carriers is larger with respect to the total number of carriers received by the terminal. At the practical demodulator SNR operating point, this DLL bias was found however to have only a negligible impact on the blind MOE BER performance. Finally, the presence of intra-beam orthogonal interference contributes to impair the effectiveness of blind-MOE interference mitigation, as it does not affect the CR but only the blind MOE by stealing signal space dimensionalities.

Figure 17 shows a set of simulation results with and without MOE in a double diversity fading channel. It appears that, notwithstanding all the above-mentioned factors contributing to degrade the effectiveness of the blind MOE receiver, its potential in reducing the negative effects of carrier unbalance[17] are quite evident. For situations with uniform carrier level, the advantages of interference mitigation are not very significant due to the strong FEC coding which actually make the operational SNIR, after despreading, very small (even less than 0 dB). At this low SNIR, thermal noise is typically dominating. Finally it shall be observed that the overall number of carriers in the example of Figure 17 is slightly larger than the spreading factor; hence the system is working in the dimensional clashing zone.

**Non-linearity Effects**

During initial modulation/spreading format trade-off, the impact of the satellite non-linearity was considered. Assuming the worst-case single SSPA for the payload non-linearity [18] it was found (see) that QPSK modulation is more sensitive to non-linearity than dual-BPSK. However, dual-BPSK also requires the double number of spreading codes and is potentially less performing in conjunction with

[17] It should be emphasized that in the forward link of a power controlled multi-beam channel, power unbalance is a typical operating condition as users situated at the beam edge will experience higher interference that the ones located inside the beam.

interference mitigation techniques. The greater sensitivity of QPSK to non-linear distortion was actually verified when the optional reference symbols were included in the traffic channels. Without the higher level optional reference symbols included in the traffic channels, the effect of non linearity was milder (see Figure 18). In this case the performance difference between the two modulation/spreading format is due to lower sensitivity of dual-BPSK to carrier phase and frequency error more than to the lower sensitivity to non-linearity. Note that the MOE detector gain versus the CR amounts to about 1.5 dB.

## B - Reverse link physical layer performance

The RL many-to-one characteristic makes it quite different from the FL. The main deviations from the FL are: I) all active mobile users will experience independent fading process, and II) no orthogonal CDMA interference occurs. As discussed previously, the RL of SW-CDMA can greatly benefit from satellite diversity. This is confirmed in Figure 19 which refers to a fast fading channel. For a slow fading channel, the advantage of diversity would have been even more significant.

In the presence of diversity, the SNR per rake finger can be significantly reduced, thus lowering the potential advantages of using linear interference mitigation techniques. Figure 20 shows some examples of the RL performance, with and without MOE. As expected, MOE is advantageous when near far effects are more significant, but power control will make their occurrence less likely.

**Nonlinearity effects**

As described previously, the SW-CDMA RL DPCCH signaling channel is multiplexed by exploiting carrier phase and code orthogonality, in order to minimize DPDCH cross-talk. This channel multiplexing technique greatly reduce envelope fluctuations [7], which represent a major drawback for a satellite terminal because the high power amplifier must operate in its nonlinear region in order to maximize the transmitted power and DC/RF efficiency and to ensure a longer battery duration. The advantages of this quadrature DPCCH insertion have been verified by evaluating the impact on the transmitted signal spectrum after MES non-linear amplification. This has been simulated using a typical solid-state amplifier. The simulated SSPA output spectrum, for a DPCCH/DPDCH power ratio equal to -6 dB (corresponding to the worst case 2.4 Kbit/s bit rate) and for an SSPA drive corresponding to the 1 dB compression point, is shown in Figure 21. The lower (dashed) power spectral density corresponds to the quadrature CDMP scheme. When compared with the power spectral density obtained without pilot

insertion, the results are very close[18], meaning that the proposed pilot insertion technique suppresses sidelobe re-growth very efficiently. More specifically, Figure 21 shows that the in-phase pilot multiplexing is characterized by an out of-band power that is 5 dB higher than that of the selected pilot insertion scheme, which significantly increases adjacent channel interference.

## C - Source coding simulations

Here we present the performance obtained by joining the proposed physical layer with audio and video telephony services. Two scenarios for digital speech coding are investigated. High quality voice is considered by using the ITU-T G.729 standard at 8 kbits/s [19]. This standard produces toll quality speech, with an algorithmic delay of only 15 msec [22]. The use of a lower quality and lower delay speech coding standard, the ITU-T G.723.1 at 6.3 kbits/s, is also simulated [23]. With both of these cases, a silence compression scheme is used to lower the bit rate during silence segments. The video telephone uses the ITU-T H.324 [24] multimedia standard to combine the G.723.1 speech at 6.3 kbits/s, and the ITU-T H.263 video at 51.2 kbits/s [25], at an overall rate of 64 kbits/s. The video telephone image format is QCIF (144 lines x 176 pixels), updated at 10 frames/s, and Annexes D, F, J, S and T are used in the coder [25].

The specific channel coding design is performed by assuming two channel coding levels. It is assumed that the inner channel convolutional decoding level (Viterbi decoder) performs hard decisions and provides the audio and video services with a bit error rate of $10^{-3}$. In order to better protect the different source coding schemes, an outer channel coding level specific to each standard is used. The choice of this second coding level is done by carefully studying the effects of the channel errors on the source decoder quality, and by establishing specific unequal error protection levels. The results of this study appear in [19]. In both the G.729 and the G.723.1-based telephony services, BCH codes are selected as outer codes [19]. These choices produce a maximum coded bit rate of 10.2 kbits/s in the G.729 case, and of 8.07 kbits/s for the G.723.1-based service. The results of the sensitivity analysis performed on the H.263 video standard have indicated that a good strategy is to protect all the coded bits evenly, at an error rate of $10^{-5}$ or better. An 8-bit (255,223) Reed-Solomon code is selected to protect all the multiplexed bits (audio, video and overhead). Video error propagation is also reduced by forcing every 16x16 pixels macroblock to be coded by transform coding, at least once every 20 frames. The videotelephony coded bit rate is

[18] The pilot-free curve was not included to preserve graph readability.

73.18 kbits/s. In order to combat the effects of the error bursts introduced by the inner Viterbi decoder and the fading channel, specific interleavers were designed for the different types of services and outer coding schemes [19].

The simulated performance of the different source coding scenarios has been evaluated by using a combination of objective and subjective measurements. The BER at the output of the outer decoder has been measured, to give an indication of the interleaver efficiency. In the case of the speech services, the segmental SNR (SEGSNR) has been computed, and subjective listening evaluations have been conducted. For the videotelephony service, a subjective evaluation has been performed. The full results appeared in [19]. Partial results are presented below. A non-frequency selective Ricean fading channel is simulated, with a Ricean factor of 10 dB. As indicated before, fast fading refers to a vehicle speed of 70 Km/h and corresponds to a Doppler spread of 140H. Slow fading corresponds to a speed of 3 Km/h and a Doppler spread of 6 Hz. All the simulations are run using the FL channel scenario.

***G.729 Speech Telephony***

The received voice quality has been evaluated, when the system is operating at threshold, i.e. when the inner Viterbi decoder delivers an average BER of around $10^{-3}$. The results, for a one minute audio passage, are given in Table 3. It is noted that the SEGSNR is always close to its largest possible value of 1.5. The degradation in voice quality, as evaluated subjectively (in informal tests), is also indicated in this table. This degradation is always small and is dominated by the burst of errors still present in the slowest fading cases. Between these error bursts, the subjective quality is high. The speech intelligibility is high at all times.

***G.723.1 Speech Telephony***

In this case, because of the limitations in the overall processing delay, the outer interleaving is limited to one voice frame. The results on voice quality, for an operation at threshold (channel BER at $10^{-3}$) are given in Table 4. Note that despite the fact that the BER performance is similar to that encountered in the G.729 scenario, the voice degradation is always high, and the speech intelligibility is deteriorated. This tends to favor the use of the G.729 standard over that of the G.723.1 standard, on a bursty channel.

***Video Telephony***

The video telephony service was evaluated for one minute sequences. The BER measured at the output of the (255,223) Reed-Solomon decoder is indicated in Table 5. These results are better than the BER

subjective threshold of $10^{-5}$ for the AWGN and the fast fading channel, but are poor for the slow fading cases. They indicate that the combination of the outer code and the outer interleaver is not powerful enough to deal with the error burst distribution typical of the slow S-UMTS channel. The subjective degradation corresponding to the cases of Table 5 is indicated in Table 6. As expected, the subjective quality is degraded in the slowest fading cases. This is particularly true for the video portion of the communications, in which even the smallest artifact is annoying. The reproduction of the audio sequence could benefit from using the G.729 standard instead of the G.723.1, although this would not comply with the H.324 multimedia standard.

The simulation results of this section show that speech telephony is possible with good quality, over all the channel scenarios at a coded bit rate of 10.2 kbits/s, by using the ITU G.729 standard. The design based on the G.723.1 standard, and operating at a coded bit rate of 8.07 kbits/s, is not satisfactory. In order to increase the quality of this latter design, either more channel resources are required, to increase the channel coding redundancy, or more delay needs to be incorporated in the system, to increase the interleaver length. Despite a powerful outer coding scheme, and a long outer interleaver, the quality of the video telephony service is acceptable only in the AWGN and the fast fading cases. Extending the operation to the slow fading scenarios would require some combination of satellite diversity, lower rate channel coding and error concealment in the video decoder. Note that double satellite diversity allows a significant drop in Eb/No for similar BERs, but that the detrimental effect of the error bursts is not significantly reduced.

## 5. Conclusions

In this paper, we presented the main results about an ESA sponsored investigation about a third generation air interface, identified as SW-CDMA, proposed for the satellite component of IMT 2000. The main SW-CDMA system features and deviations from T-UMTS W-CDMA proposal have been discussed jointly with satellite system peculiarities impacting the physical layer. Some simulation results for the forward and RL of the proposed SW-CDMA air-interface have been reported and discussed. In addition to physical layer basic performance over typical fading channels, the advantages provided by satellite path diversity, blind linear CDMA interference mitigation techniques and power control have been illustrated in few typical system configurations. The impact of typical forward and RL non-linearity have been simulated. Physical layer results have been complemented by end-to-end simulation including the audio/video source codec showing the relation between operation SNIR, BER and quality of service.

Summarizing, it has been shown that with a limited number of adaptations the satellite UMTS component can benefit from the ongoing terrestrial UMTS standardization and development effort. In this framework, ESA is actively supporting the development and demonstration of an open S-UMTS air interface maximizing the commonality with the emerging T-UMTS standard. It is felt that this approach may eventually lead to a successful and truly complementary S-UMTS component development.

# References


[1] ITU IMT-2000 Radio Proposals server: http://www.itu.int/imt/2-radio-dev/proposals/index.html – See also ITU IMT-2000 Radio Reports server http://www.itu.int/imt/2-radio-dev/reports/index.html

[2] B. Lyons, B. Mazur, J. Lodge, M. Moher, S. Crozier, L. Erup, *"A High Capacity Third-Generation Mobile Satellite System Design"*, European Trans. On Telecommunications, vol. 9, No. 4, July/August 1998.

[3] European Space Agency Contract No. 12497/NL/97/NB, *"Robust Modulation and Coding for Personal Communication Systems"*, Space Engineering (I), ASCOM Systec (CH), Square-Peg.Inc. (CDN), Communication Research Canada (CDN), Politecnico of Torino (I), University of Rome Tor Vergata (I).

[4] E. Lutz, D. Cygan, M. Dippold, F. Dolainsky, W. Papke, *"The Land Mobile Satellite Channel - Recording, Statistics and Channel Model*", IEEE Trans. on Vehic. Techn. Vol. VT - 40, May 1991.

[5] Y. Karasawa et al., *"Analysis of Availability Improvement in LMSS by Means of Satellite Diversity Based on Three-State Propagation Channel Model*", IEEE Trans. on Vehicular Technol., Nov. 1997.

[6] G.E. Corazza, C. Caini, "S*atellite Diversity Exploitation in Mobile Satellite CDMA Systems*", submitted to the IEEE Wireless Communication and Networking Conf., WCNC '99, New Orleans, Sept. 21-24, 1999.

[7] G.E. Corazza and R. De Gaudenzi, *"Pilot-Aided Coherent Uplink for DS-CDMA Satellite Networks"*, IEEE Trans. on Comm., Vol. 48, No. 5, May 1999.

[8] G.E. Corazza, "*On the MAX/TC Criterion for Code Acquisition and Its Application to DS-SSMA Systems*", IEEE Trans. on Communications, Vol. 44, No. 9, pp. 1173-1182, Sep. 1996.

[9] M.K. Sust et al., *"Rapid Acquisition Concept for Voice Activated CDMA Communication"*, Proc. IEEE Globecom 1990, San Diego (CA), USA.

[10] G.E. Corazza, A. Vanelli Coralli, "*Burst vs. Continuous Pilot Acquisition in Wideband CDMA Cellular mobile Systems*", Proc. Of the IEEE Wireless Communications and Networking Conference, WNCN'99, New Orleans, Sep. 21-24, 1999.

[11] R. De Gaudenzi, F. Giannetti, M. Luise, *Signal Recognition and Signature Code Acquisition in CDMA Mobile Packet Communications*, IEEE Trans. on Vehic. Technology, Vol. 47, No. 1, Feb. 1998.

[12] M. Honig, U. Madhow, S. Verdu', *"Blind Adaptive Multiuser Detection"*, IEEE Trans. On Inform. Theory, vol. 41, No. 4, July, 1995.

[13] U. Madhow, *"Blind Adaptive Interference Suppression for Direct-Sequence CDMA"*, Proc. of the IEEE, VOL. 86, NO. 10, October 1998, pp. 2049-2069.

[14] R. De Gaudenzi, J. Romero-Garcia, F. Giannetti, M. Luise, *"A Frequency Error Resistant Blind Interference Mitigating CDMA Detector"*, IEEE 1998 Fifth International Symposium on Spread-Spectrum Techniques and Applications, Sun City, South Africa, September 1998.

[15] Centro TEAM and SGS-Thomson Microelectronics, *"Multi User Interference Cancellation Demodulator"*, ESA Contract No. 13095/98/NL/SB.

[16] J. Romero-Garcia, R. De Gaudenzi, *"On Antenna Design and Capacity Analysis for the FL of a Multi-beam Power Controlled Satellite CDMA Network"*, Subm. to IEEE Jour. on Sel. Areas in Comm., 1999

[17] F. Adachi et al., *"Tree Structured Generation of Orthogonal Spreading Codes with Different Length for the FL of DS-CDMA"*, Electronics Letters, Vol . 33, No. 1, pp. 27-28.

[18] R. De Gaudenzi, *"Globalstar Paylaod Nonlinearity Effects on the FL CDMA Multiplex: Part I; Physical Layer Analysis"*, IEEE Trans. on Vehic. Tech., May 1999.

[19] W. R. Braun, *"PN Acquisition and Tracking Performance in DS/CDMA Systems with Symbol Length Spreading Sequences"*, IEEE Trans. on Comm. , Vol. T-COM 45, No. 12, Dec. 1997, pp. 1595-1601.

[20] D. Boudreau, R. Lyons, G. Gallinaro, R. De Gaudenzi, *"A Simulation of Audio and Video Telephony Services in a Satellite UMTS Environment"*, in the Proc. of the International Mobile Satellite Communication Conference '99, Ottawa, Canada, June 1999.

[21] International Telecommunication Union, *Coding of Speech at 8 kbit/s using Conjugate-Structure Algebraic-Code-Excited Linear Prediction (CS-ACELP)*, ITU-T Recommendation G.729 (03/96), March 1996.

[22] R. V. Cox, *Three new speech coders from the ITU cover a range of applications*, IEEE Communications Magazine, vol. 35, no. 9, September 1997, pp. 40-47.

[23] International Telecommunication Union, *Dual rate speech coder for multimedia communications transmitting at 5.3 and 6.3 kbit/s*, ITU-T Recommendation G.723.1 (03/96), March 1996.

[24] International Telecommunication Union, *Terminal for low bit-rate Multimedia Communication*, ITU-T Recommendation H.324 (02/98), February 1998.

[25] International Telecommunication Union, *Video Coding for Low Bitrate Communication*, ITU-T Recommendation H.263 (02/98), February 1998.

[26] R. De Gaudenzi, C. Elia, R. Viola, *"Band-Limited Quasi-Synchronounous CDMA: A Novel Multiple Access Technique for Personal Communication Satellite Systems"*, IEEE Journ. on Sel. Areas in Comm., Vol. 10, No. 2, February 1992.

[27] G. Caire, R. De Gaudenzi, G. Gallinaro, R. Lyons, M. Luglio, M. Ruggieri, A. Vernucci, H. Widmer, *"ESA Satellite Wideband CDMA Radio Transmission Technology for the IMT-2000/UMTS Satellite Component: Features & Performance"*, subm. to IEEE GLOBECOM '99, Rio De Janeiro, Brazil, 5-9 December 1999.

[28] G. Caire, R. De Gaudenzi, G. Gallinaro, R. Lyons, M. Luglio, M. Ruggieri, A. Vernucci, H. Widmer, *"Development and Validation of a Wideband CDMA IMT-2000 Physical Layer for Satellite Applications"*, Proc. IMSC '99, Ottawa, Canada, June 1999.

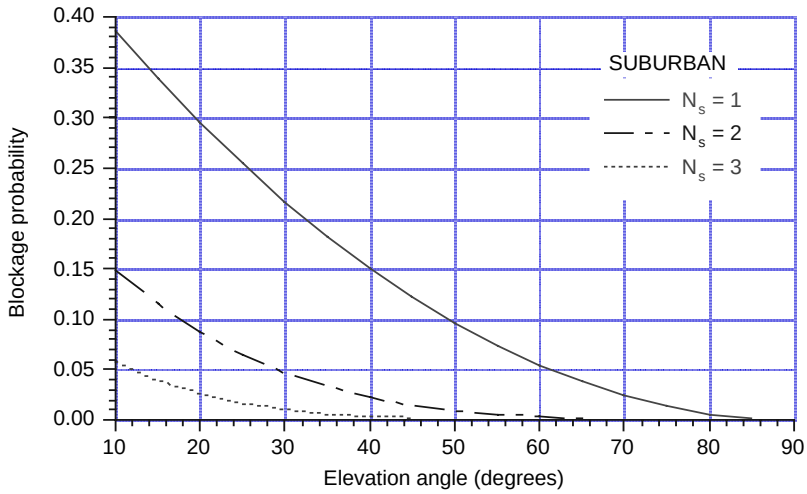


**Figure 1:** *Path blockage probability in a suburban area, with the number of satellites ($N_s$) above the minimum elevation angle as a parameter [6].*

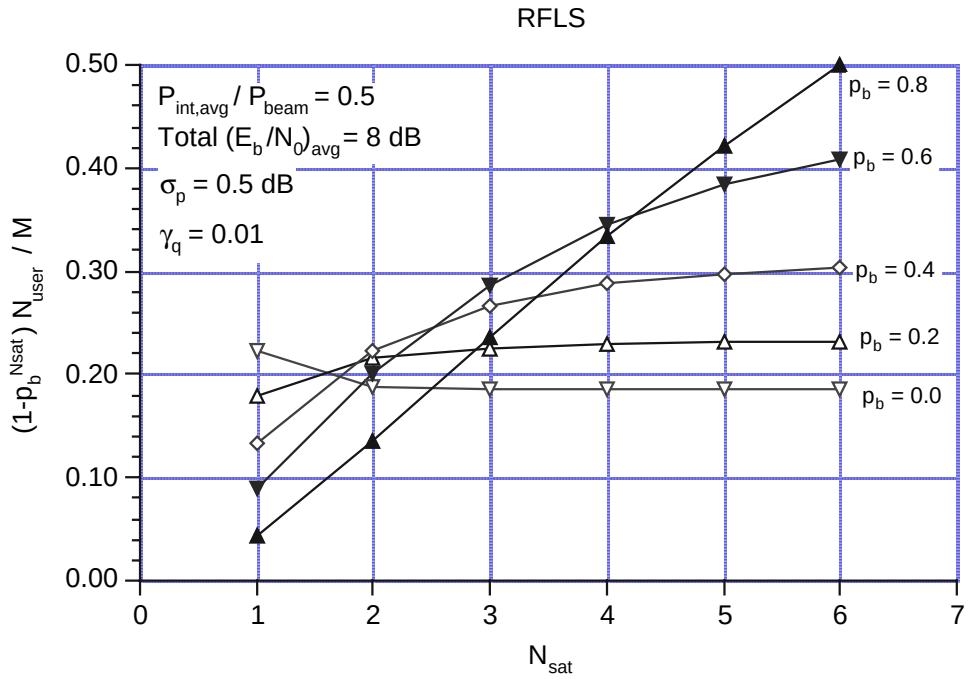


**Figure 2:** *Product of system capacity and probability of at least one clear link versus the number of satellite in visibility [$N_{sat}$], with the single path blockage probability [$p_b$] as a parameter. 50 % interfering power from other (same satellite) beams, power control error standard deviation $\sigma_p$=0.5 dB, outage probability $\gamma_b=10^{-2}$.*

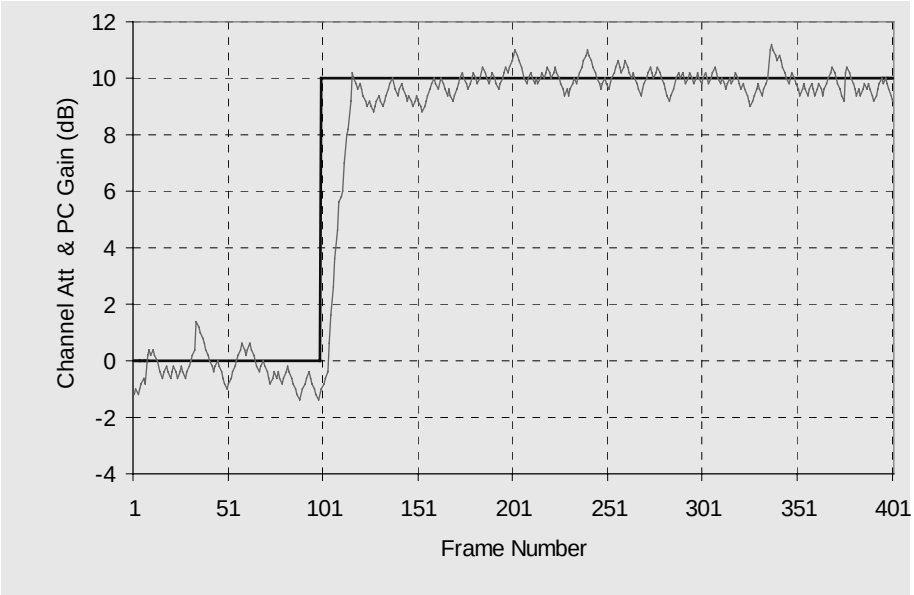


**Figure 3:** *Power control loop response to a 10 dB step attenuation (AWGN channel). Loop delay is 120 ms. gain steps are 0.2 and 1 dB.*

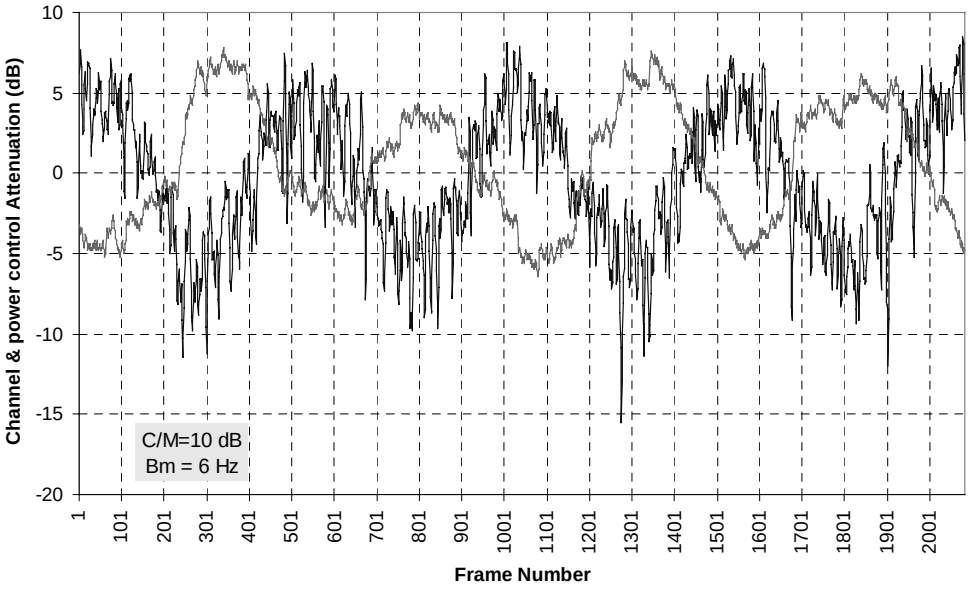


**Figure 4:** *Power control loop response to a 10 dB peak-to peak sinusoidal variation (frequency 0.1 Hz) superimposed to a Ricean fading (C/M=10 dB, Doppler spread = 6 Hz). Loop delay is 120 ms., gain steps are 0.2 dB and 1 dB.*

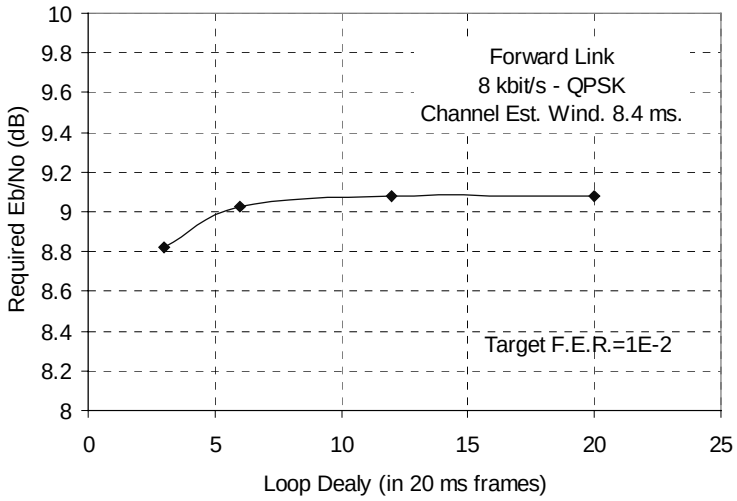


**Figure 5:** *Required Eb/No for F.E.R.=$10^{-2}$ as a function of the loop delay (bi-level power control gain step=0.5 dB) for a slow fading case (Doppler spread= 6 Hz).*

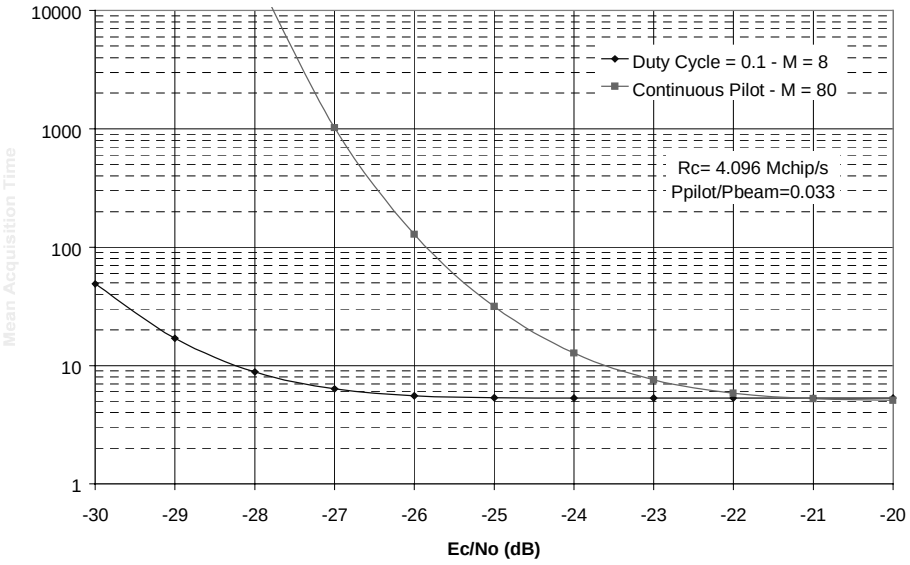


Figure 6: ***FL mean acquisition time (ms.) versus pilot thermal $E_C/N_0$ for a continuous and bursty pilot. Average pilot power equal to 3.3% of the total beam power. M is the number of post integration. The assumed duty cycle for the bursty pilot correspond to one code period out of ten transmitted.***

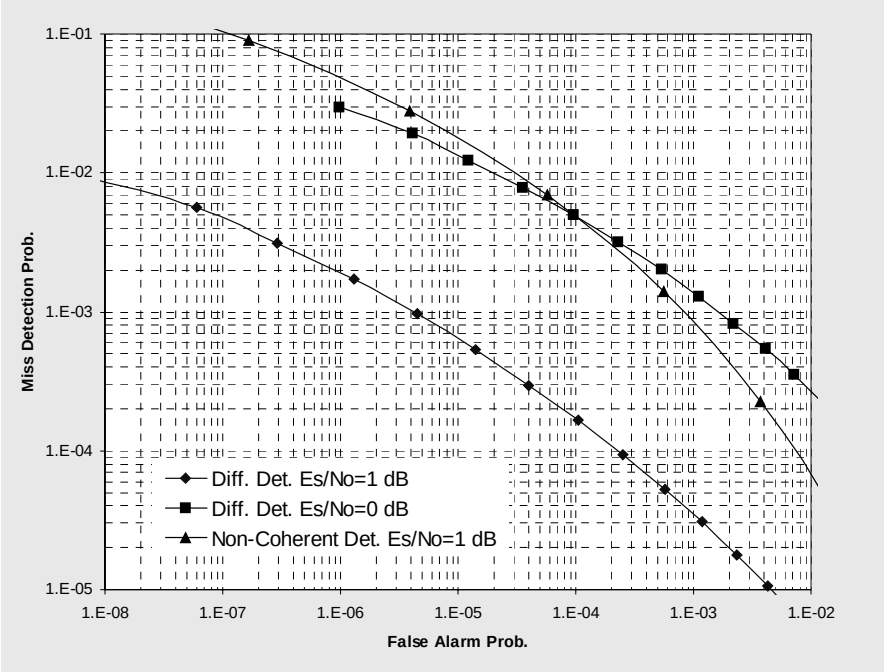


**Figure 7:** *ROC for differential detection of a 48 symbols UW. $E_s/(N_0+I_0)$ equal to 0 and 1 dB. Also shown is the ROC for non-coherent detection over 49 symbols.*

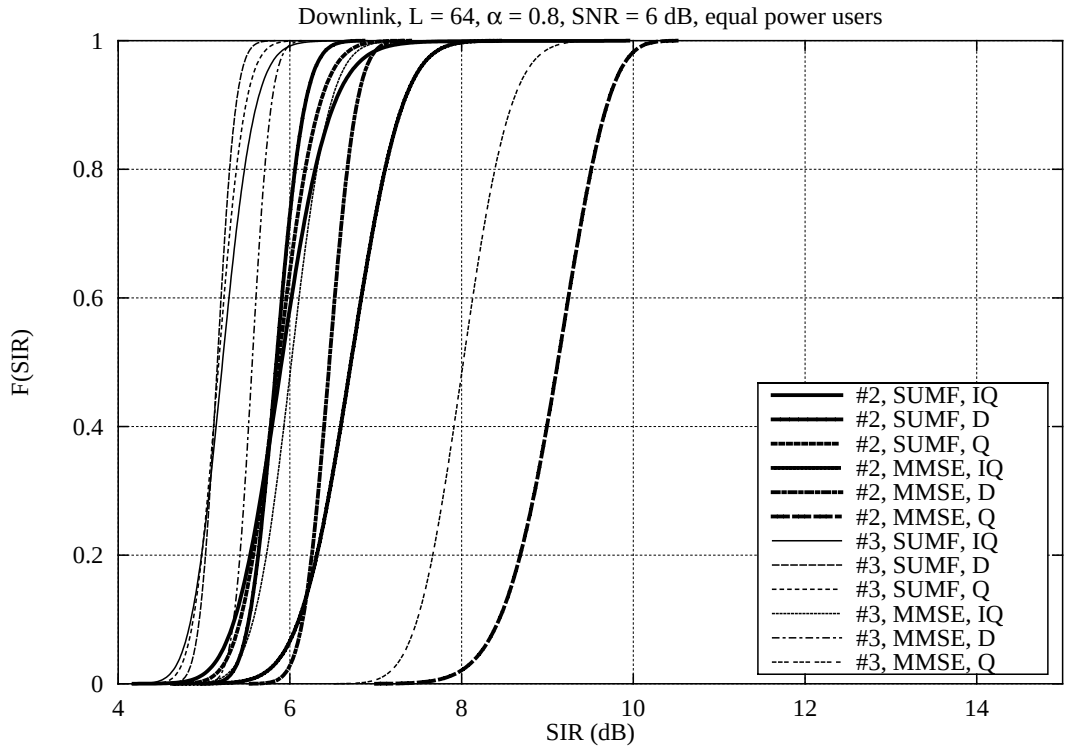


Figure 8: ***FL SIR cumulative distribution function. Number of users/spreading factor=0.8.***

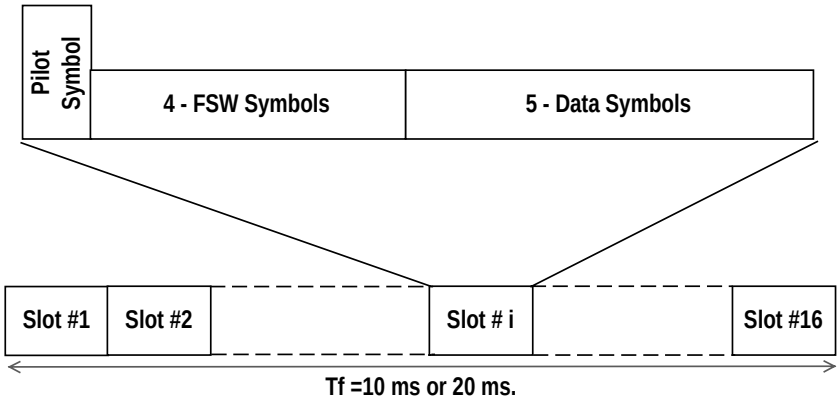


**Figure 9:** ***Primary Common Control Physical Channel***

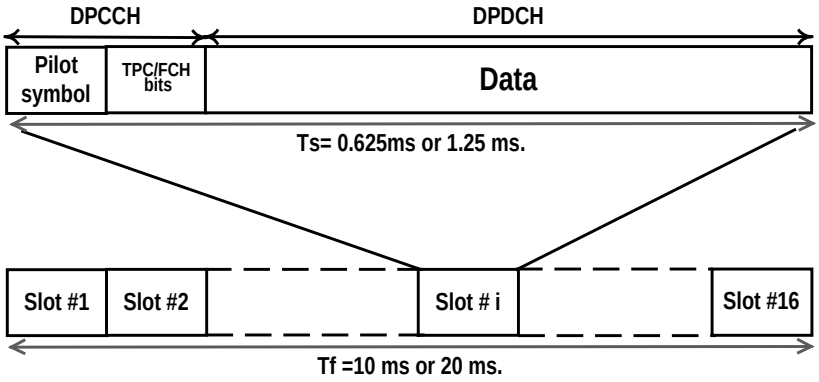


a) FL

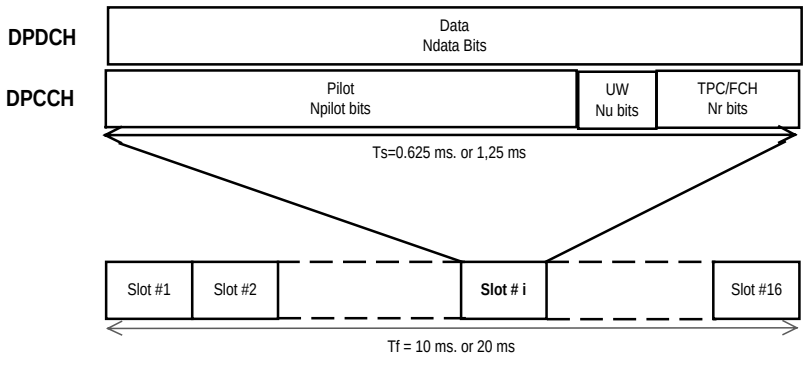


b) return link

**Figure 10:** *Frame Structure of the Forward and Return Link Dedicated Physical Channels (DDPCH/DCPCH).*

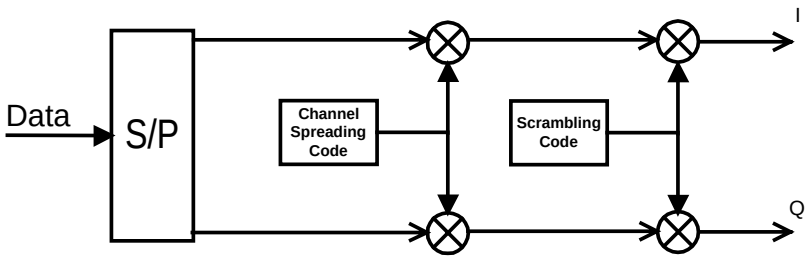


**Figure 11: FL modulation and spreading**

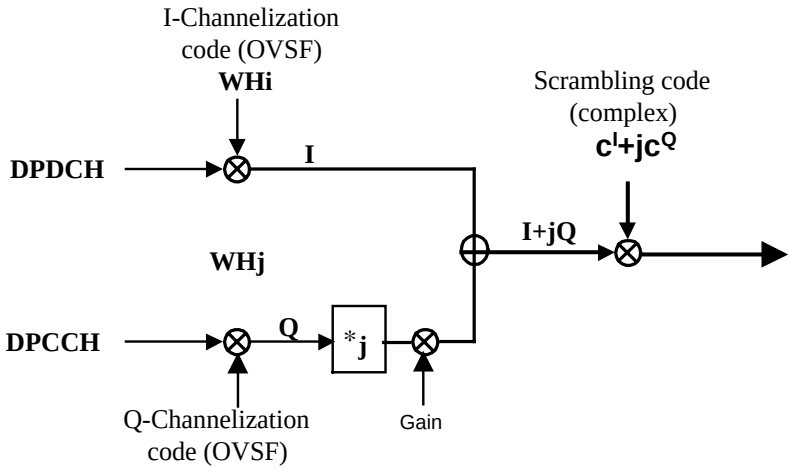


**Figure 12:** *RL modulation and spreading*

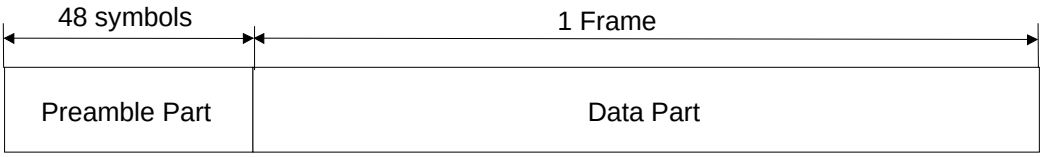


**Figure 13:** ***PRACH channel structure***

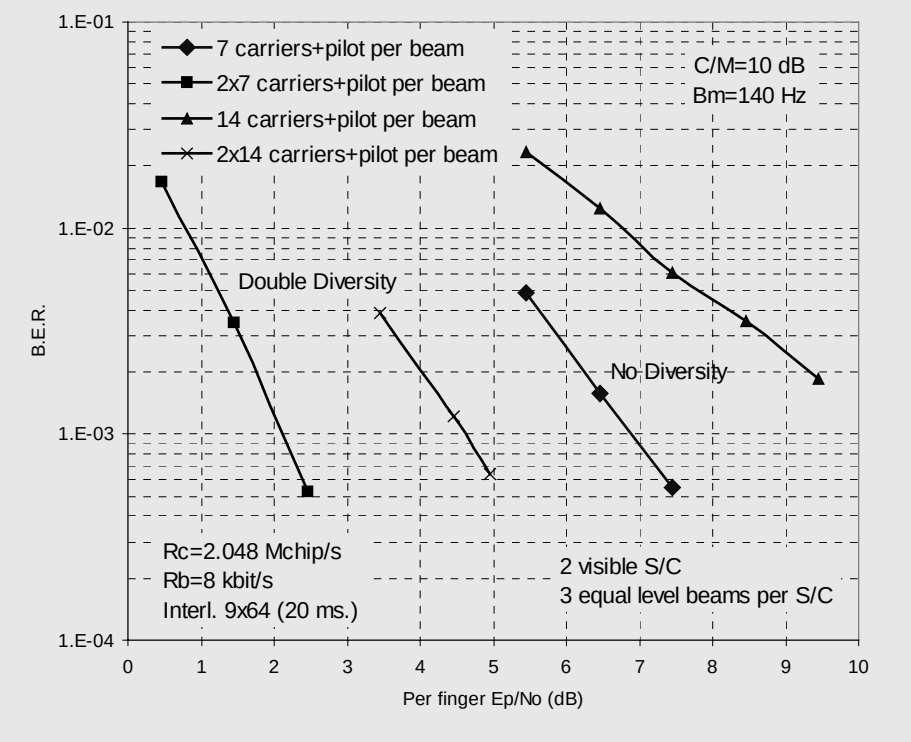


**Figure 14:** *Performance in single and double diversity with a conventional receiver. Fast fading case.*

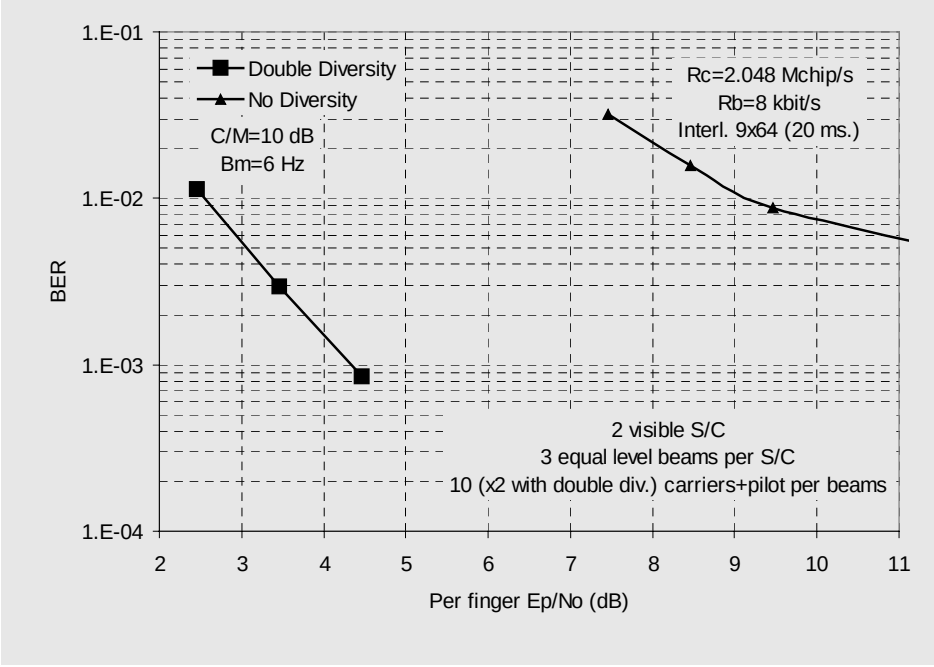


**Figure 15:** *Performance in single and double diversity with a conventional receiver. Slow fading case.*

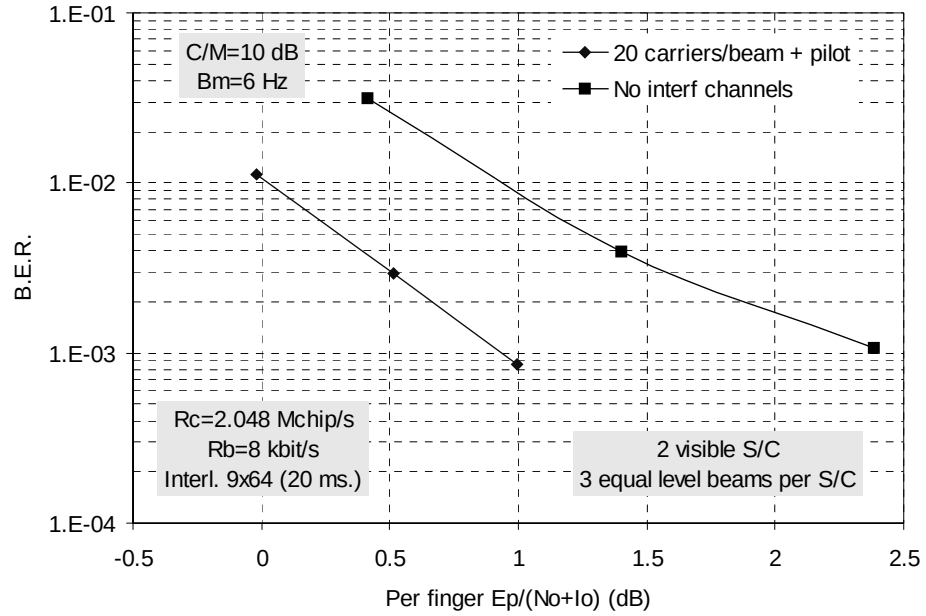


**Figure 16:** *Results with slow fading and double diversity versus thus the overall $E_b/(N_0+I_0)$ in two different interference scenario. Reference symbols are not included in the DPCCH.*

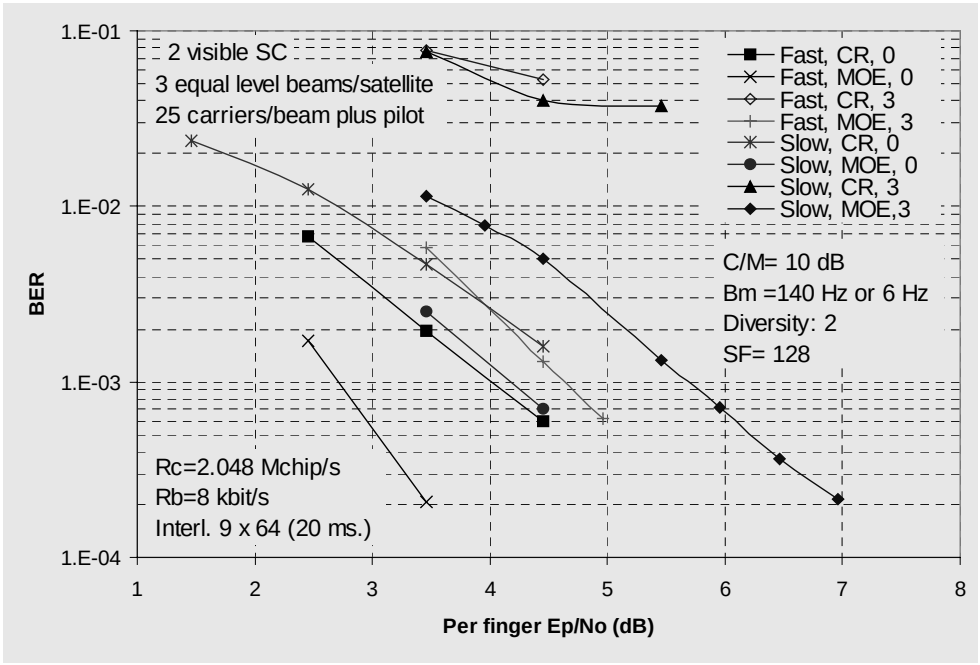


**Figure 17:** *BER performance with MOE in a double satellite diversity. The wanted user receives three beams per satellite at the same level. Each beam (including wanted) carries 25 carriers plus the pilot. Interfering carriers are either @ 0 or +3 dB level with respect to wanted carriers. Reference symbols only on PCCPCH (+6 dB level with respect to other symbols). Blind-MOE algorithm windows size = 2 symbol.*

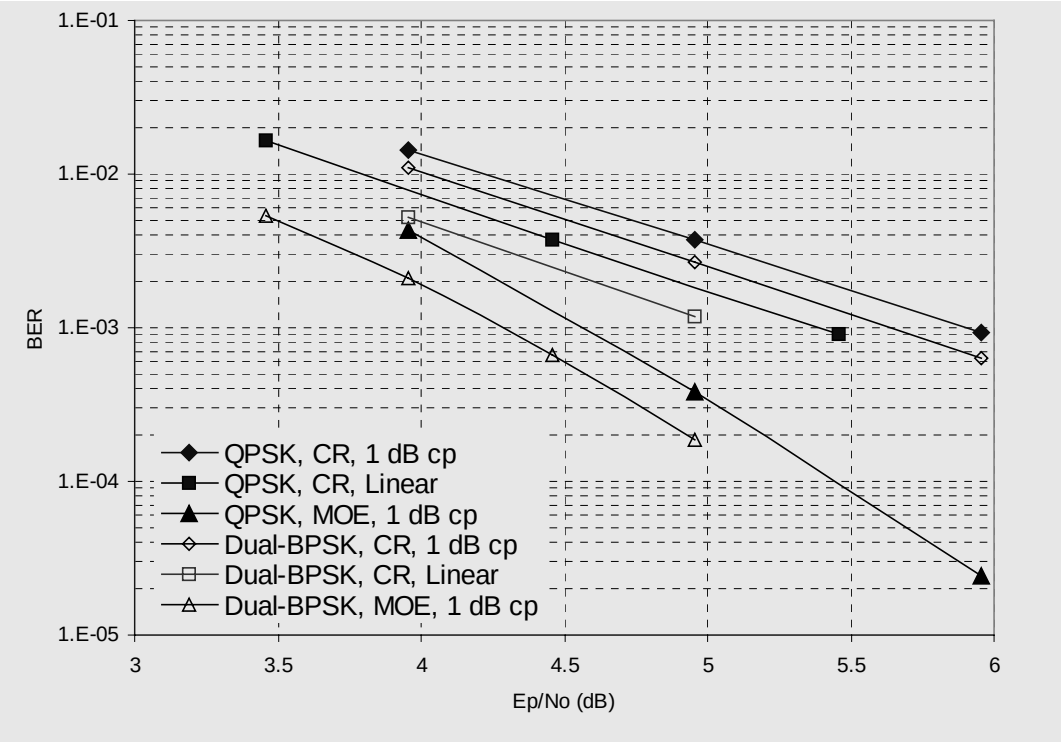


**Figure 18:** *Non-Linearity effects on performance. The simulated case correspond to an AWGN channel with 12 synchronous interfering carriers and 40 asynchronous interfering carriers, all having the same level as the wanted carrier.*

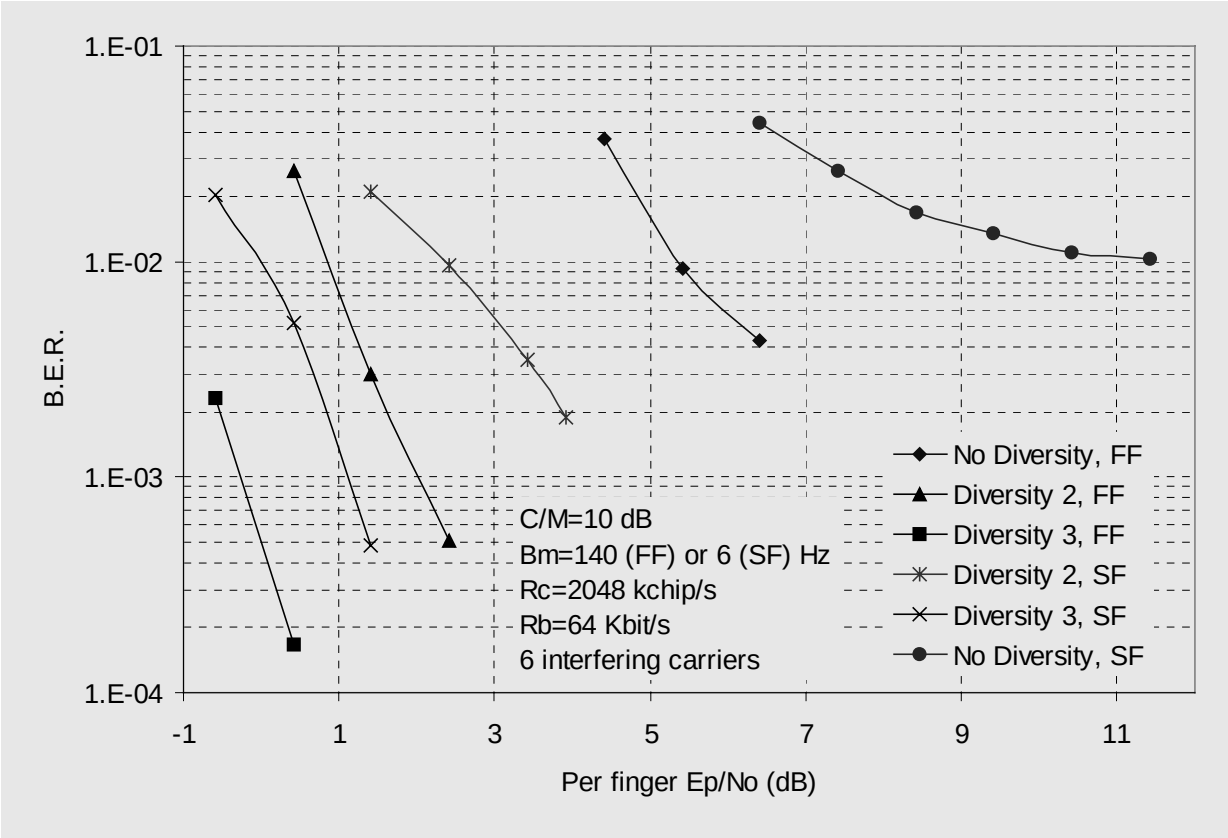


**Figure 19:** *Fast and slow fading RL BER with diversity 1, 2, 3 and CR detector. Interfering carriers have the same level as the wanted one. The DPCCH power is 10% of that of the DPDCH. The basic FEC coding is r=1/2.*

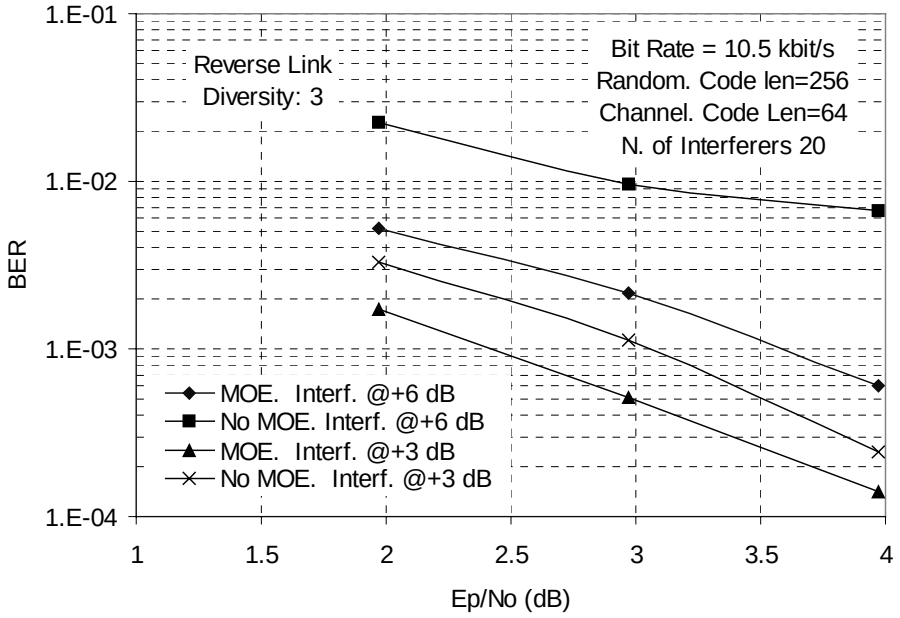


**Figure 20:** *RL BER with and without Blind MOE detector. The number of interfering channel was 20 with relative level with respect to the wanted carrier of 3 dB or 6 dB.*

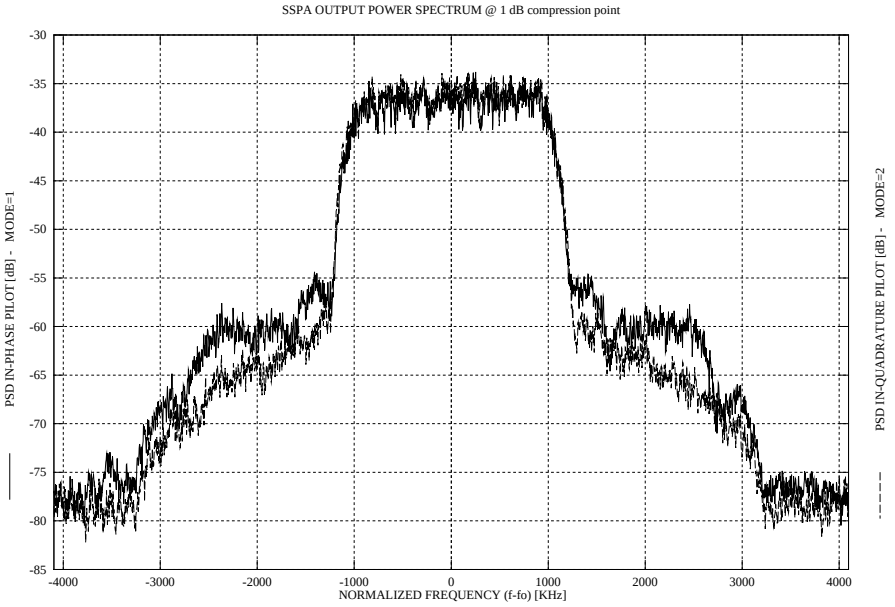


**Figure 21:** *Simulated transmitted signal power flux density for DPCCH/DPDCH power ratio equal -6 dB [2.4Kb/s], MES SSPA @ 1 dB compression point: a) continuous line: in-phase DPCCH, b) dash-dotted line: SW-CDMA with quadrature DPCCH.*

| | $A_{pp}$ | $E_b/N_0$ | FER | BER |
|---|---|---|---|---|
| No Power Control | 5 | 7.17 | 4.0 e-3 | 2.87e-4 |
| With Power Control | 5 | 7.34 | 1.21e-2 | 1.21e-3 |
| No Power Control | 10 | 9.17 | 2.31e-2 | 2.25e-3 |
| With Power Control | 10 | 9.14 | 1.17e-2 | 1.12e-3 |

**Table 1:** *Average Eb/No requirement with a 5 or 10 dB peak-to peak ($A_{pp}$) sinusoidal variation (frequency 0.1 Hz) superimposed to a Ricean fading (C/M=10 dB, Doppler spread = 140 Hz). Loop delay is 120 ms., gain step is 0.5 dB (bi-level loop).*

| Logical Channels | Link direction | Physical Channels |
|---|---|---|
| Broadcast Control Channel (BCCH) | Forward | Primary Common Control Physical Channel (Primary CCPCH) |
| Forward Access Channel (FACH)<br>Paging Channel (PCH) | Forward<br>Forward | Secondary Common Control Physical Channel (Secondary CCPCH) |
| Random Access Channel (RACH)<br>Random Traffic Channel (RTCH) | Reverse | Physical Random Access Channel (PRACH) |
| Dedicated Control Channel (DCCH) | Forward/Reverse | Dedicated Physical Data Channel (DPDCH) |
| Dedicated Traffic Channel (DTCH) | Forward/Reverse | Dedicated Physical Data Channel (DPDCH) |
| Layer 1 signaling | Forward/Reverse | Dedicated Physical Control Channel (DPCCH) |

**Table 2:** ***Mapping of Logical Channels to Physical Channels***

| Channel | Eb/No (dB) | SEGSNR (dB) | Subjective Degradation | Intelligibility |
|---|---|---|---|---|
| AWGN | 4 | 1.41 | small | high |
| Fast fading (140 Hz) | 6 | 1.42 | small | high |
| Slow fading (6 Hz) | 9 | 1.44 | small | high |
| Slow fading with double satellite diversity | 4 | 1.45 | small | high |

**Table 3:** *G.729 objective voice quality (SEGSNR) and the subjective degradation for a channel BER of $10^{-3}$. The error-free SEGSNR is 1.5 dB. The degradation scale is: none, small, medium and high.*

| Channel | Eb/No (dB) | SEGSNR (dB) | Subjective Degr. | Intelligibility |
|---|---|---|---|---|
| AWGN | 3.5 | 9.16 | high | medium |
| Fast fading (140 Hz) | 5.75 | 10.18 | high | medium |
| Slow fading (6 Hz) | 8.5 | 10.38 | high | medium |
| Slow fading with double satellite diversity | 4 | 10.5 | high | medium |

**Table 4:** *G.723.1 objective voice quality (SEGSNR) and the subjective degradation for a channel BER of $10^{-3}$. The error-free SEGSNR is 10.97 dB. The degradation scale is: none, small, medium and high.*

| Channel | Eb/No (dB) | Outer BER on R-S Decoded Bits |
|---|---|---|
| AWGN | 3 | $< 1x10^{-10}$ |
| Fast fading (140 Hz) | 4.5 | $< 1x10^{-10}$ |
| Slow fading (6 Hz) | 8 | $8x10^{-4}$ |
| Slow fading with double satellite diversity | 4 | $4x10^{-4}$ |

**Table 5:** *The measured BER at the output of the (255,223) Reed-Solomon decoder in the video telephony service, for a channel BER of $10^{-3}$.*

| Channel | *Audio* Subjective Degradation | *Video* Subjective Degradation |
|---|---|---|
| AWGN | none | none |
| Fast fading (140 Hz) | none | none |
| Slow fading (6 Hz) | high | high |
| Slow fading with double satellite diversity | high | high |

**Table 6:** *The subjective degradation for the cases of Table 5. The degradation scale is: none, small, medium and high.*